Electronic Transduction of Photostimulated Binding Interactions at Photoisomerizable Monolayer Electrodes: Novel Approaches for Optobioelectronic Systems and Reversible Immunosensor Devices

Itamar Willner* and Bilha Willner

Institute of Chemistry, The Hebrew University of Jerusalem, Jerusalem 91904, Israel

Photoisomerizable monolayers assembled onto electrode supports act as "command interfaces" for controlling the binding interactions of biomaterials with the functionalized surfaces. The light-induced binding and dissociation of the biomaterials to and from the electrodes, respectively, are electronically transduced. Two systems, including the photostimulated binding and dissociation of cytochrome *c* (Cyt *c*) and of anti-DNP antibody to and from functionalized surfaces, are discussed. The application of the systems as optobioelectronic devices and reversible immunosensors is addressed. A mixed monolayer consisting of pyridine and nitrospiropyran (**1a**) photoisomerizable units assembled on a Au-electrode acts as a command interface for the light-controlled association and dissociation of Cyt *c* to and from the monolayer. Cyt *c* binds to the pyridine/**1a**-monolayer electrode, resulting in electrical contact between the redox protein and the electrode. Photoisomerization of the mixed monolayer to the pyridine/protonated merocyanine state (**1b**) results in the electrostatic repulsion of Cyt *c* and its dissociation from the electrode support. This blocks the electrical contact between Cyt *c* and the electrode. By the cyclic photoisomerization of the mixed monolayer between the **1a** and **1b** states, reversible "ON"−"OFF" amperometric transduction of the affinity interactions between the redox protein and the interface is accomplished. Coupling of the photostimulated electrical contact between Cyt *c* and the electrode surface to the Cyt *c*-mediated bioelectrocatalyzed reduction of O_2 by cytochrome oxidase provides a means to amplify the transduced electronic signal. A photoisomerizable thiolated dinitrospiropyran (**2a**) monolayer, assembled on solid supports, acts as a light-active antigen interface that enables the photocontrolled binding and dissociation of anti-dinitrophenyl antibody (DNP-Ab) to and from the interface. The dinitrospiropyran (**2a**) layer acts as an antigen for the DNP-Ab, whereas the protonated dinitromerocyanine (**2b**) lacks antigen features for the DNP-Ab. By reversible photoisomerization of the monolayer between the **2a** and **2b** states, cyclic binding and dissociation of DNP-Ab to and from the monolayer interface is accomplished. The association and dissociation of the DNP-Ab to and from the **2a**- and **2b**-monolayer states are electronically transduced, using amperometric, Faradaic impedance and microgravimetric, quartz crystal microbalance analyses. The photostimulated binding of an antibody to a photoisomerizable antigen monolayer provides a novel method to design reversible immunosensor devices.

The integration of biomaterials with electronic transducer supports and the electronic transduction of biological events, such as binding or catalysis occurring at the transducer surface, are the basic features of bioelectronic and biosensor systems (*1, 2*). Electrical contacting of enzymes with electrodes and bioelectrocatalytic activation of the proteins provide the fundamental principles of many biosensor devices (*3*−*6*). Electrical (*7, 8*) or piezoelectrical (*9, 10*) transduction of the formation of antigen−antibody complexes at electrodes or quartz crystals enabled the organization of immunosensors. Similarly, the formation of double-stranded oligonucleotide−DNA complexes was electronically transduced by oligonucleotide-functionalized electrodes (*11*) or piezoelectric crystals (*12*). Integration of photoswitchable biomaterials with electronic transducers provides a general means to develop future optobioelectronic systems. In these systems, light-stimulated biological events occurring at the transducer element, such as binding or catalysis, are electronically transduced and, eventually, amplified in the form of an electronic output such as current, potential, impedance, or piezoelectric crystal frequency signals. Chemical modification of redox enzymes with photoisomerizable units generates photoswitchable electrobiocatalysts, and their integration with electrode supports enables the amplified amperometric transduction of photonic signals recorded by the biomaterial. For example, chemical modification of glucose oxidase with photoisomerizable nitrospiropyran units (*13*) or the reconstitution of apo-glucose oxidase with a semisynthetic nitrospiropyran−FAD cofactor (*14*) yields photoswitchable biocatalysts. Integration of the photo-

* Tel: 972-2-6585272. Fax: 972-2-6527715. E-mail: willnea@vms.huji.ac.il.

10.1021/bp990115a CCC: $18.00
Published on Web 11/03/1999

Scheme 1. Photoswitchable Binding and Dissociation of a Biomaterial to and from a Command Interface Composed of a Photoisomerizable Layer Associated with a Transducer[a]

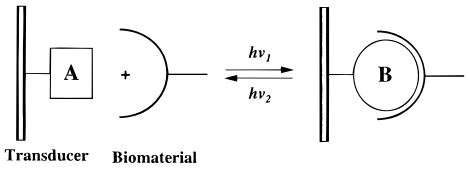

[a] $h\nu_1$ and $h\nu_2$ represent different light energies required to photoisomerize the light-sensitive components.

Scheme 2. Photoswitchable Binding and Dissociation of a Charged Biomaterial to and from a Photoisomerizable Monolayer[a]

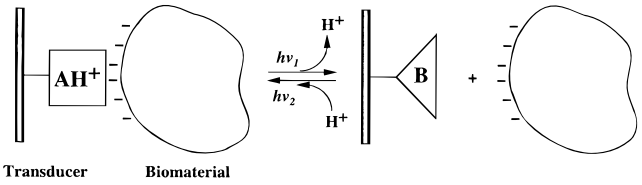

[a] $h\nu_1$ and $h\nu_2$ correspond to the light energies used for the photoisomerization of the monolayer.

switchable redox enzymes with electrode supports, enabled the electrical transduction of the light-activated bioelectrocatalytic reactions.

A different approach to tailor optobioelectronic systems involves the chemical modification of the transducer with a photosensitive monolayer or thin film that acts as a "command interface" for controlling the binding of the protein to the transducer element. This regulates the electrical contact or the electrocatalytic features of the biomaterial, and the electronic transduction of the light-stimulated biological events is accomplished (*15*). Scheme 1 outlines the concept of a command interface by the assembly of a photoisomerizable monolayer on an electrode support and control of the binding of a redox protein onto the transducer. In the photoisomer state A of the monolayer, no affinity for the protein exists, and no electrical contact with the redox protein is attained. Photoisomerization to state B generates an interface that attracts and binds the redox protein to the transducer. This results in the electrical contact of the redox enzyme with the electrode and the amperometric transduction of the photonic signal recorded by the monolayer. The interactions between the biomaterial and the command-interface-supported transducer might be electrostatically attractive, Scheme 2. In the positively charged photoisomer state of the photosensitive interface, the negatively charged biomaterial is attracted and concentrated at the electronic transducer, whereas in the complementary photoisomer state of the command interface, no attractive interaction exists. For example, a nitrospiropyran photoisomerizable monolayer assembled onto an electrode was reported to act as a command interface for the control of the electrical contact of ferrocene-tethered glucose oxidase with the electrode support (*15*). In the nitrospiropyran-monolayer state, no affinity interaction between the biocatalyst and the electrode exists, resulting in the inefficient bioelectrocatalyzed oxidation of glucose. Photoisomerization of the monolayer to the protonated merocyanine state leads to the electrostatic attraction of the biocatalyst to the electrode support and its concentration at the conductive support. This effects the efficient bioelectrocatalyzed oxidation of glucose and the amplified amperometric transduction of the light signal that was recorded (absorbed) by the monolayer and stimulated the isomerization process.

In the present article, we address the organization of optobioelectronic systems based on photostimulated binding processes between photoisomerizable command surfaces and proteins. The association (or dissociation) of a biomaterial, e.g., protein, onto (or from) an electronic support could lead to different physicochemical consequences on the interfacial properties of the transducer. Association of a redox protein onto an electrode could lead to the electrical contact of the biocatalyst with the conductive support, and the light-stimulated binding event could then be amperometrically transduced. Photochemical binding of a protein onto a functionalized surface, e.g., an antibody, yields an insulating layer on the electrode support. This is anticipated to control the impedance features as well as the interfacial electron-transfer properties at the electrode surface. Thus, light-induced binding (or dissociation) of a protein at a photosensitive command interface could be transduced by impedance spectroscopy (*16*) or by the indirect characterization of the electron-transfer properties of a redox probe in the electrolyte phase. Binding or dissociation of proteins to and from the photosensitive functionalized interface effects microgravimetric changes at the transducer element. As a result, by the application of piezoelectric crystals, e.g., quartz crystal microbalance, as the transducing unit, the photostimulated binding or dissociation events are electronically transduced by frequency changes in the crystal. In the present report we demonstrate the use of different electronic transduction means of photostimulated bioaffinity interactions at functionalized electrodes. Specific emphasis is directed to the development of optobioelectronic systems and reversible immunosensor devices.

Results and Discussion

Photostimulated Binding of Cytochrome *c* at a Photoisomerizable Pyridine-Monolayer-Functionalized Electrode. Cytochrome *c* (Cyt *c*) usually lacks direct electrical communication between the redox-active heme sites and electrodes. Functionalization of the electrode with pyridine molecular units (*17, 18*) or other molecular components (*19, 20*) generates binding sites for Cyt *c* on the electrode support, resulting in the alignment of the hemoprotein and the promotion of electrical contact. Because Cyt *c* is a positively charged protein at neutral pH environments (*21*), we attempted to photoregulate the electrical communication between the hemoprotein and the electrode, using the electrostatically controlling command interface principle (*22*), Scheme 3. A mixed monolayer consisting of thiol nitrospiropyran (**1a**), photosiomerizable units, and pyridine components was assembled onto a Au-electrode. Figure 1, curve a, shows the cyclic voltammogram of Cyt *c* in the presence of the pyridine/nitrospiropyran mixed-monolayer-functionalized electrode. The quasireversible electrochemical response indicates effective electrical communication between the heme site of Cyt *c* and the electrode. This electrical contact is attributed to the association of the hemoprotein and alignment of the redox center onto the electrode. Photoisomerization of the monolayer to the protonated merocyanine state (**1b**, MRH^+-state) blocks the electrical contact between Cyt *c* and the electrode, Figure 1, curve b. This is attributed to the electrostatic repulsion of Cyt *c* from the electrode support. By reversible photoisomerization of the monolayer-functionalized electrode between the SP- and MRH^+-states in the presence of Cyt *c*, the electrode responses can be cycled

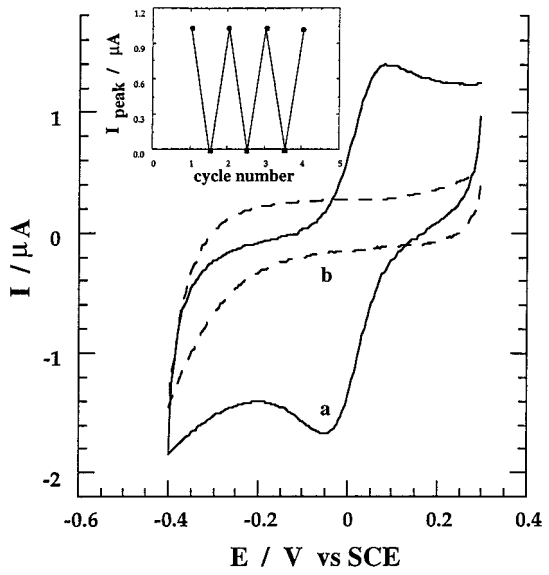

Figure 1. Cyclic voltammogram of Cyt *c*, 1×10^{-4} M, in the presence of the (a) thiol-pyridine nitrospiropyran monolayer electrode (generated by irradiation at $\lambda > 475$ nm) and (b) thiol-pyridine-protonated nitromerocyanine monolayer electrode (generated by irradiation at $400 > \lambda > 360$ nm). Data recorded in electrolyte solution composed of Na_2SO_4, 0.1 M, and phosphate buffer, 0.01 M, pH = 7.0; scan rate 50 mV s^{-1}. Inset: cyclic amperometric transduction of the association and dissociation of Cyt *c* upon reversible photoisomerization of the monolayer electrode.

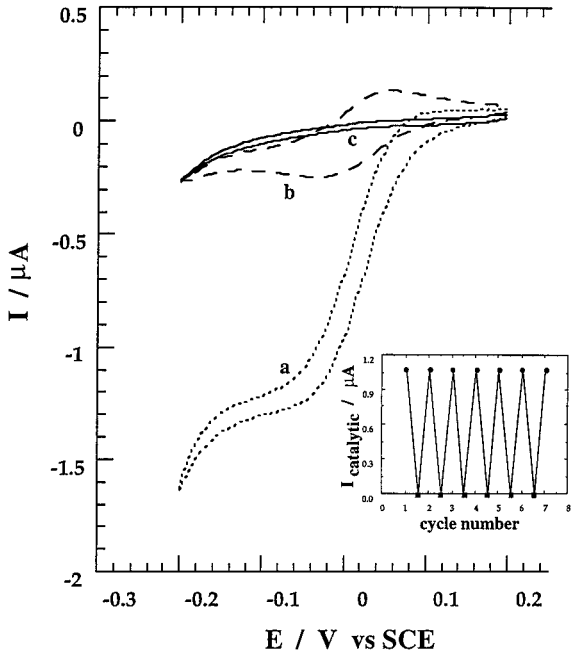

Figure 2. Cyclic voltammogram of (a) the Cyt *c*/COx/O_2 system in the presence of the thiol-pyridine-nitrospiropyran mixed monolayer electrode, (b) Cyt *c* alone in the presence of the thiol-pyridine-nitrospiropyran monolayer electrode, and (c) the Cyt *c*/COx/O_2 system in the presence of the thiol-pyridine-protonated nitrospiropyran monolayer electrode. In all experiments: Cyt *c*, 1×10^{-4} M; COx, 1×10^{-6} M; electrolyte composition Na_2SO_4, 0.1 M, phosphate buffer, 0.01 M, pH = 7.0; scan rate 2 mV s^{-1}. Inset: cyclic amperometric transduction of the bioelectrocatalyzed reduction of O_2 by the Cyt *c*/COx system upon reversible photoisomerization of the monolayer electrode.

between a high amperometric response, switch "ON", and a mute, switch "OFF", respectively, Figure 1, inset.

Cytochrome *c* acts as a versatile electron-transfer mediator that activates many electrocatalyzed transformations. Thus, conjugation of the electrically contacted Cyt *c*-functionalized electrode-integrated assembly with a Cyt *c*-dependent enzyme is anticipated to stimulate a bioelectrocatalytic transformation. Activation of the bioelectrocatalytic cascade transformation provides a means to amplify the electrical communication event between the Cyt *c* and the electrode. That is, the bioelectrocatalytic turnover mediated by Cyt *c* results in an electrocatalytic current that reflects the primary electronic contact between the hemoprotein and the conductive support. Cytochrome oxidase (COx) was coupled to the Cyt *c*- functionalized electrode system as a biocatalyst for the Cyt *c*-mediated reduction of oxygen, Scheme 3. Figure 2, curve a, shows the cyclic voltammogram of the Cyt *c*/COx/O_2 system in the presence of the nitrospiropyran/pyridine mixed-monolayer configuration. For comparison, the cyclic voltammogram of Cyt *c* alone, in the absence of COx, is shown in Figure 2, curve b. A clear electrocatalytic cathodic current is observed with COx. Control experiments reveal that no electrocatalytic current is observed in the absence of Cyt *c*, implying that the bioelectrocatalyzed reduction of O_2 is mediated by the electrically contacted Cyt *c*. It is also evident that in the presence of the COx/O_2 biocatalytic cascade, the primary electrical communication of Cyt *c* is amplified through the enzymatic reaction. Photoisomerization of the monolayer to the protonated merocyanine configuration (MRH^+-state) results in the electrostatic repulsion and dissociation of Cyt *c* from the electrode. This blocks the electrical contact between the hemoprotein and the electrode, and the secondary electrocatalytic reduction of O_2 is inhibited, Figure 2, curve c. By cyclic photoisomerization of the monolayer between the SP- and MRH^+-configurations, the amperometric responses of the electrode are reversibly switched between "ON" and "OFF" states, Figure 2, inset. The "ON" state corresponds to the amplified amperometric transduction of the photonic signal that is recorded by the monolayer and induces the isomerization of the monolayer interface.

Scheme 3. Photostimulated Association and Dissociation of Cyt *c* to and from a Thiol-Pyridine/Nitrospiropyran Mixed Monolayer Associated with a Au-Electrode and Secondary Light-Induced Activation of the Bioelectrocatalyzed Reduction of O_2 by COx

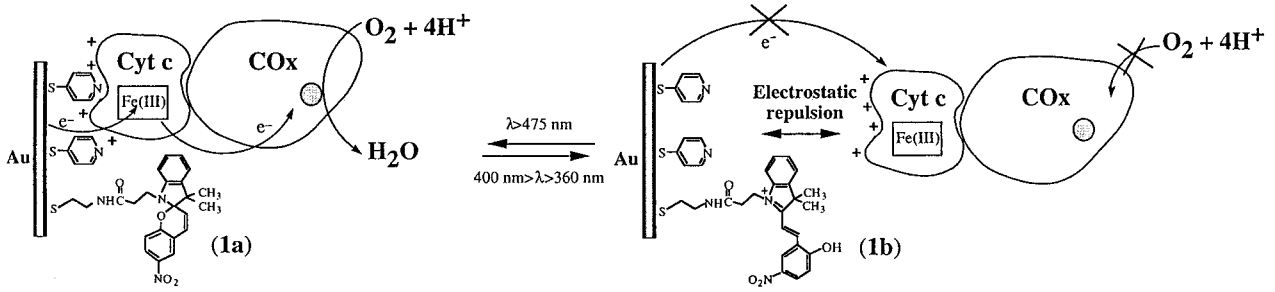

Scheme 4. Schematic Function of the Vision Process[a]

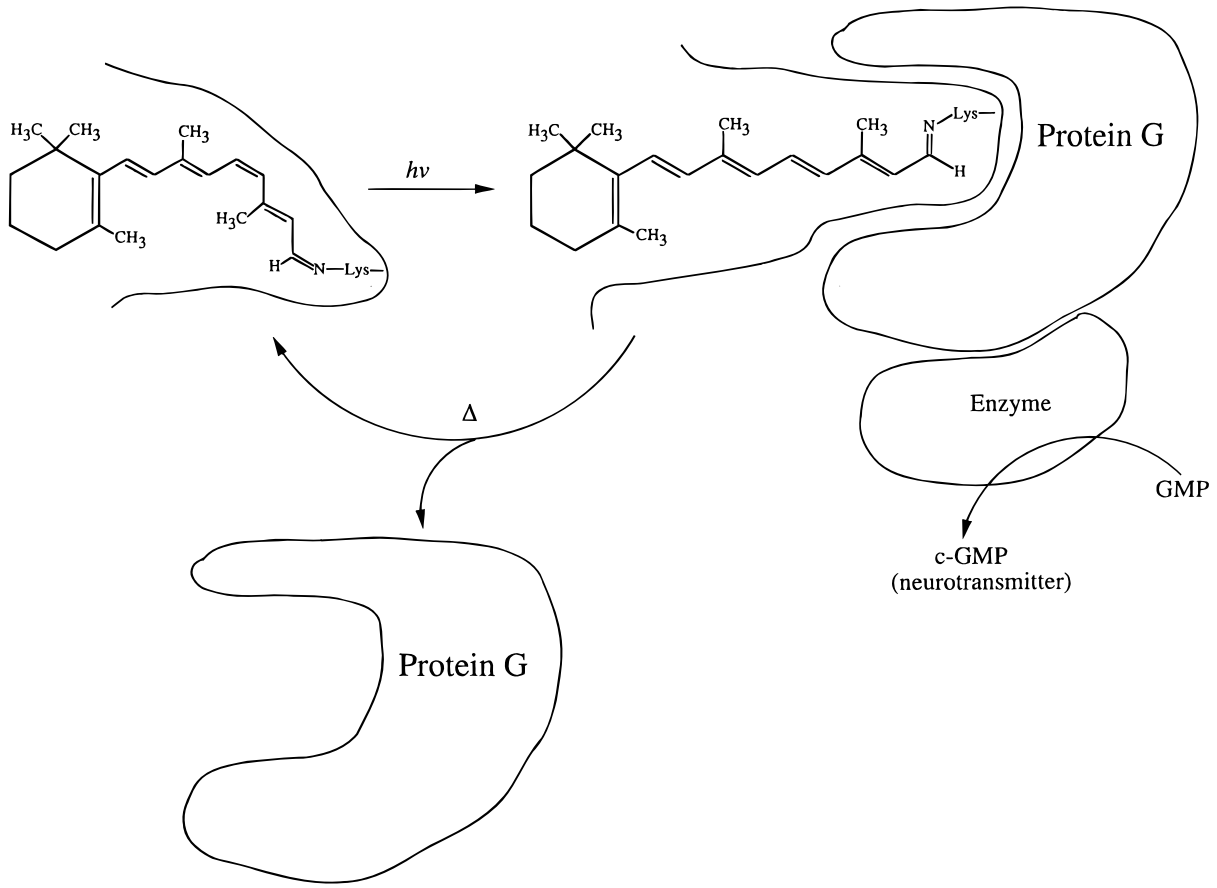

[a] Δ corresponds to thermal isomerization.

The photoswitchable electrobiocatalytic system consisting of the photoisomerizable monolayer electrode and Cyt *c*/COx/O_2 mimics functions of the vision apparatus. In the vision process, 11-*cis* to 11-*trans* photoisomerization of the retinal chromophore induces a conformational change in the surrounding protein, Scheme 4. This structural perturbation of the protein results in the binding of Protein G to the photogenerated binding site. Bound Protein G acts as a messenger that activates the enzyme cascade, generating c-GMP. This latter product is the neurotransmitter that initiates the neural response of the vision process. Relaxation of the retinal chromophore to its initial 11-*cis* configuration releases the Protein G, and the synthesis of c-GMP is blocked. The photochemical bioelectrocatalytic assembly consisting of the photoisomerizable monolayer electrode and the Cyt *c*/COx/O_2 system duplicates functions of the native vision process. The mixed monolayer, consisting of nitrospiropyran/pyridine units, is analogous to the retinal protein microenvironment. Cytochrome *c* mimics the functions of Protein G. Photoisomerization of the monolayer interface to the neutral nitrospiropyran state stimulates the binding of Cyt *c* to the electrode support. Association of Cyt *c* onto the electrode facilitates the electrical contact between the hemoprotein and the electrode, and this activates the enzyme cascade of COx/O_2, analogous to the synthesis of c-GMP. The analogy we address between the synthetic nitrospiropyran/pyridine-functionalized electrode integrated with Cyt *c*/COx/O_2, suggests future potential applications of this man-made optobioelectronic device. The system enables the storage of photonic information and its transduction as an amplified amperometric output and represents a Read−Write−Store system. The photonic triggering of the current response and the amplification of the optical signal with the transduced amperometric output allow the use of the system as a photonic amplifier and sensitive actinometer.

Photostimulated Binding of anti-DNP Antibody at a Photoisomerizable Dinitrospiropyran-Monolayer-Functionalized Transducer. An alternative approach to fabricate photoactive command surfaces for the electronic transduction of photonic signals involves the light-induced generation of binding sites for the biomaterial on the transducer, Scheme 1. This method will be addressed here with the development of optobioelectronic systems for the association/dissociation of an antibody to and from a functionalized photoactive antigen layer assembled on the transducer element. In one configuration of the monolayer, state A, the interface lacks antigen properties for the antibody, and no affinity interactions exist between the support and the antibody. Photoisomerization of the monolayer to state B, Scheme 1, yields an interface exhibiting antigen features for the antibody, and the antigen−antibody complex is formed on the transducer. By the appropriate design of an electronic element, it recognizes and transduces the formation of the antigen−antibody complex at the solid support, and the optoelectronic sensing device for the antibody is tailored. This photochemical immunosensor device has an important feature of reversibility that enables the light-induced regeneration of the sensor interface (*23*), as schematically outlined in Scheme 5. The transducer is functionalized with the photoisomerizable antigen. The monolayer in photoisomer state A exhibits

Scheme 5. Photostimulated Binding and Dissociation of an Antibody to and from a Photoisomerizable Antigen Monolayer Assembled on a Transducer; Deisgn of a Reversible Immunosensor

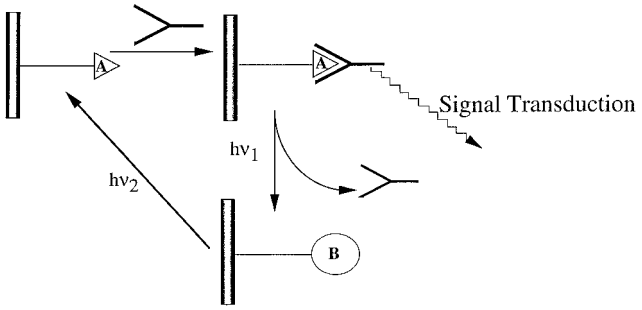

antigen properties for the antibody, and formation of the antigen−antibody complex is electronically transduced by the system. After completion of the sensing cycle, the interface is photoisomerized to state B, which lacks antigen features for the antibody. This enables the wash-off of the antibody and the dissociation of the primary antigen−antibody affinity complex. Further photoisomerization of the layered interface to state A regenerates the active antigen layer. This two-step irradiation process establishes a cycle for the reuse and regeneration of electronic immunosensor systems (*23*).

We will address three different electronic transduction means for sensing the formation and dissociation of the antigen−antibody complexes at the transducer element. These will include the amperometric, impedometric, and piezoelectrical probing of the antigen−antibody interactions at the solid support. The photoisomerizable sensing interface was organized by the assembly of the mercaptobutyl dinitrospiropyran (**2a**) on Au-electrodes or Au-electrodes associated with a piezoelectric quartz crystal (9 MHz, AT-cut), Scheme 6. The monolayer exhibits reversible photoisomerizable features, and photoirradiation of the dinitrospiropyran monolayer (**2a**, SP-state) yields the protonated dinitromerocyanine layer (**2b**, MRH^+-state), whereas visible light irradiation of the monolayer restores the SP-state. The photoisomerizable molecular components exhibit the appropriate photoswitchable antigen properties for the anti-dinitrophenyl antibody (DNP-Ab). The dinitrospiropyran isomer acts as antigen for the DNP-Ab, while the protonated dinitromerocyanine lacks antigen properties or affinity for the DNP-Ab (*24*). Scheme 7 presents several electronic transduction means of the photoswitchable association and dissociation of the DNP-Ab to and from the photoisomerizable antigen monolayers associated with the respective transducer elements. These include Faradaic impedance and cyclic voltammetry as electrochemical transduction signals and microgravimetric, quartz crystal microbalance (QCM) analyses. The electrochemical transduction is based on the electrical insulation of the electrode support toward a redox probe in solution upon binding of the DNP-Ab to the monolayer interface. The QCM transduction is based on mass changes occurring on a piezoelectric crystal upon the binding of the DNP-Ab to the antigen monolayer and subsequent control of the crystal frequency. (For detailed discussion of the methods, see below).

Impedance spectroscopy is an effective method to probe the interfacial features of modified electrodes. Not only is the impedance spectrum an electronic transduction signal for the surface properties of the electrode, but theoretical analysis (*25, 26*) of the spectrum enables the understanding of fundamental chemical transformations associated with the conductive electrode. Formation of the antigen−antibody complex at the electrode surface is anticipated to perturb the capacitance and resistance of the electrode−eletrolyte interface, and hence impedance measurements could reflect the formation of the antigen−antibody complex at the electrode. Indeed, impedance spectroscopy was used to probe the formation of antigen−antibody complexes (*27*) or biotin−avidin affinity structures (*28*).

In an impedance experiment, a low-amplitude sinosoidal voltage is applied to the electrochemical cell, and the resulting current response is measured. The impedance is calculated as the ratio of the system potential phasor, $U(j\omega)$, and the current phasor, $I(j\omega)$, that are generated by a frequency response analyzer, eq 1, where $j = \sqrt{-1}$,

$$Z(j\omega) = U(j\omega)/I(j\omega) = Z_{re}(\omega) + jZ_{im}(\omega) \qquad (1)$$

f corresponds to the excitation frequency (rad s^{-1}), and $\omega = 2\pi f$ (Hz).

The complex impedance of the system is presented by the sum of the real, $Z_{re}(\omega)$, and imaginary, $Z_{im}(\omega)$, components that originate from the resistance and capacitance of the cell, respectively. The electronic circuit equivalent to the impedance features of the cell is depicted in Scheme 8. It includes the resistance of the electrolyte solution, R_s, the Warburg impedance Z_w, originating from the diffusion of ions from the bulk solution to the electrode interface, the double-layer capacitance, C_{dl}, and the electron-transfer resistance, R_{et}. The latter component is important when a redox probe is solubilized in the electrolyte solution and a resistance for interfacial electron transfer exists. For any modified electrode and particularly for a monolayer electrode consisting of an antigen−antibody complex layer, a barrier for electron transfer exists, Scheme 7. That is, the binding of the antibody to the antigen layer generates a thick (∼80−120 Å) insulating layer that perturbs the interfacial electron transfer. Thus, photoswitchable binding or dissociation of the antibody to and from the photoisomerizable antigen monolayer electrode is anticipated to be transduced by significantly different Faradaic impedance signals. The Faradaic current in the presence of a solubilized redox probe and the corresponding component of the impedance, Z_{re}, will significantly contribute to the resulting impedance spectrum. The theoretical impedance spectrum (*25*) presented as the Nyquist plot (Z_{im} vs Z_{re}) is expected to include a semicircle lying on the Z_{re} axis continued by a straight line. The semicircle portion observed at higher frequencies corresponds to the electron-transfer-limited process, whereas the linear part is characteristic for lower-frequency domains and the diffusionally limited process. The electron transfer kinetic parameters and the diffusional characteristics can be extracted from the semicircle and linear parts of the impedance spectra, respectively (*25*). The semicircle diameter is equal to the electron-transfer resistance, R_{el}, and the intercept of the semicircle with the Z_{re} axis at high frequencies corresponds to the electrolyte solution resistance, R_s. Extrapolation of the circle to lower frequencies yields the intercept that is equal to $R_s + R_{el}$. The maximum value of the imaginary impedance in the semicircle region corresponds to $Z_{im} = R_{et}/2$ and is achieved at ω_o given by eq 2. The electron-transfer

$$\omega_o = (C_{dl}R_{et})^{-1} \qquad (2)$$

Scheme 6. Assembly of a Dinitrospiropyran Photoisomerizable Antigen Monolayer on a Au-support and Light-Induced Switchable Interactions of DNP-Ab with the Photoisomerizable Monolayer

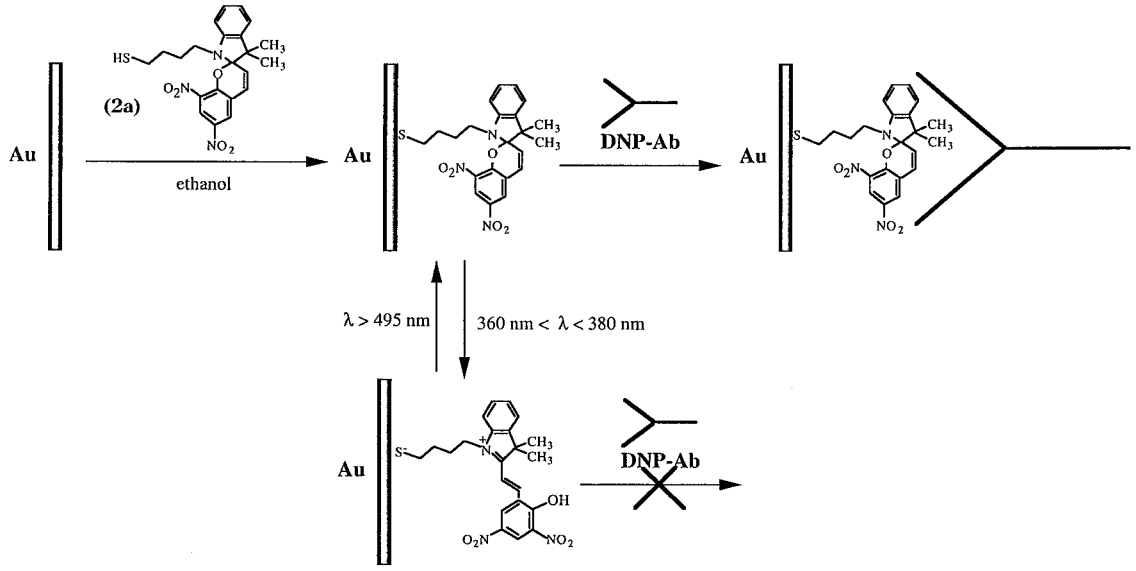

Scheme 7. Electornic Transduction of Photoswitchable Interactions of the DNP-Ab with the Photoisomerizable Dinitrospiropyran Monolayer Assembled on Transducer Elements[a]

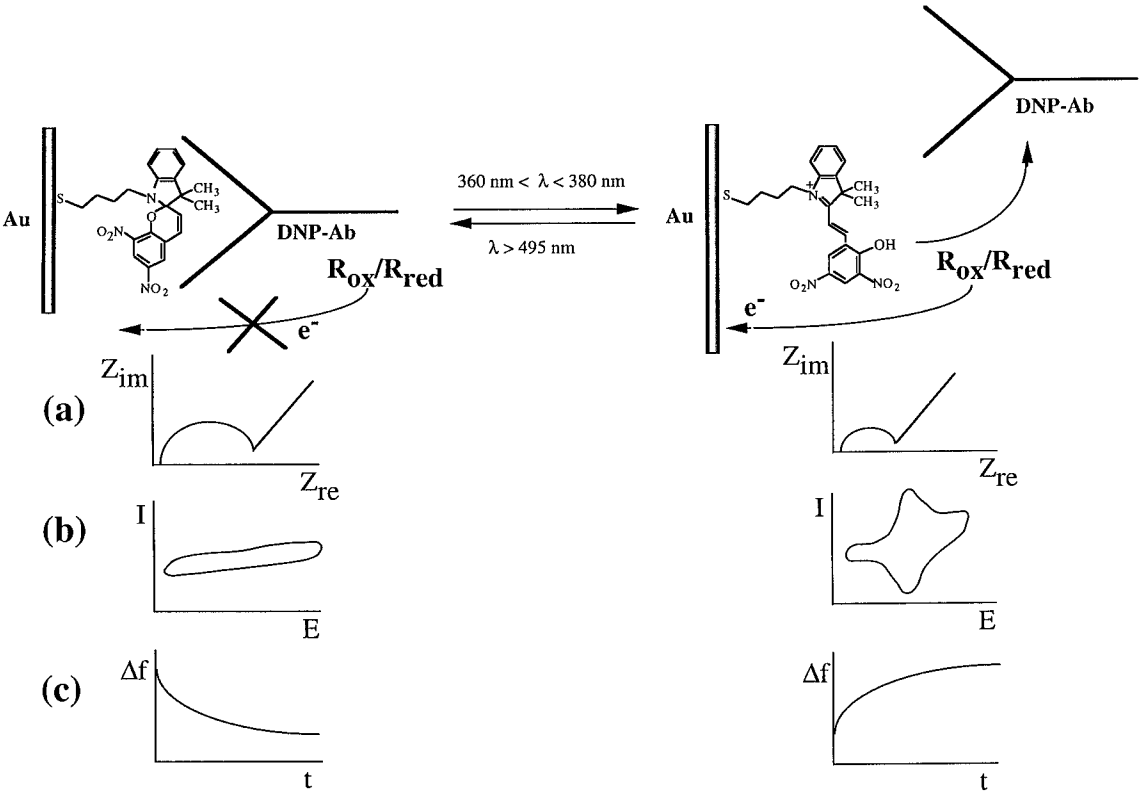

[a] (a) Using Faradaic impedance transduction (Z_{im} and Z_{re} correspond to the imaginary and real impedance components). (b) Using cyclic voltammetry (I and E correspond to the current and potential values, respectively). (c) Using microgravimetric, quartz crystal microbalance (QCM) analysis (Δf and t correspond to the crystal frequency change and time, respectively).

resistance can be translated into the exchange current under equilibrium, I_o, eq 3. The heterogeneous electron-

$$R_{et} = RT(nFI_o)^{-1} \quad (3)$$

transfer rate constant, k_{et}, can be evaluated by taking into account the dependence of k_{et} on the applied potential, eq 4, where [S] is the bulk concentration of the redox

$$I_o = nFAk_{et}[S]\exp(-\alpha nF\Delta E/RT) \quad (4)$$

Scheme 8. Equivalent Circuit for the Impedance Spectrum Corresponding to the Association of an Antibody to an Antigen-Monolayer-Functionalized Electrode

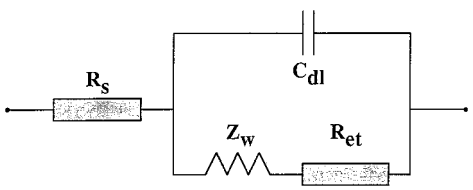

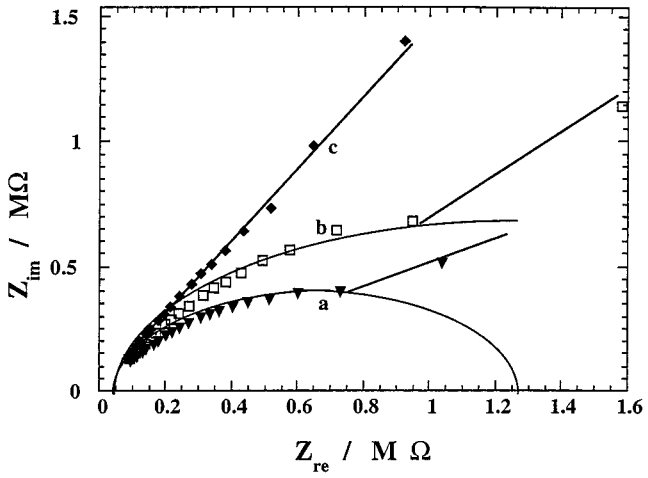

Figure 3. Nyquist diagram (Z_{im} vs Z_{re}) for the Faradaic impedance of (a) protonated dinitromerocyanine (**2b**)-monolayer electrode (generated by irradiation at $380 > \lambda > 360$ nm), (b) dinitrospiropyran (**2a**)-monolayer electrode (generated by irradiation at $\lambda > 495$ nm), and (c) dinitrospiropyran (**2a**)-monolayer electrode upon addition of DNP-Ab. All experiments were performed in the presence of Fc-GOx, 3 mg mL^{-1}, and glucose, 1×10^{-1} M, in 0.01 M phosphate buffer, pH = 7.0. The applied bias constant potential was 0.4 V; amplitude of alternating voltage was 10 mV.

probe, α is the electron-transfer coefficient, and ΔE is the applied potential. Thus, the association of the antibody to the photoisomerizable dinitrospiropyran antigen monolayer electrode is anticipated to induce a high electron-transfer resistance, R_{et}, in the presence of a redox probe solubilized in the electrolyte. This process will be reflected with a large-diameter semicircle region in the impedance spectrum of the system. Photoisomerization of the monolayer to the protonated dinitromerocyanine configuration and dissociation of the DNP-Ab will facilitate the interfacial electron transfer, and the lowered electron-transfer resistance will be reflected by a smaller semicircle diameter in the resulting impedance spectrum, Scheme 7a.

The redox probe that we have employed for probing the Faradaic impedance spectra of the photoisomerizable dinitrospiropyran monolayer electrode is glucose oxidase tethered with ferrocene units (Fc-GOx) and glucose as the enzyme substrate. Glucose tethered with ferrocene units is electrically contacted with electrodes and mediates the bioelectrocatalyzed oxidation of glucose (*15*, *29*). The macromolecular ferrocene-tethered glucose oxidase was selected as redox probe because the interfacial electron transfer between the Fc-GOx and the electrode is anticipated to be blocked upon association of the DNP-Ab and the interfacial electron-transfer characteristics are insensitive to microscopic defects of the monolayer. Such microscopic surface defects might still provide diffusional paths for molecular redox probes that might perturb the insulating features and the resulting electron-transfer resistance of the antigen−antibody complex. Figure 3, curves a and b, shows the Faradaic impedance spectra of the photoisomerizable monolayer electrode in the presence of the bioelectrocatalytic system Fc-GOx/glucose. (Impedance spectra were recorded with an electrochemical impedance analyzer, EG & G 6310, and spectra are plotted in the form of the Nyquist diagram, Z_{im} vs Z_{re}). The impedance spectra follow the theoretical shape and include a semicircle lying on the Z_{re} axis continued by a straight line. The semicircle domain, observed at high frequencies, corresponds to the electron-transfer-limited process, whereas the linear part, characteristic of the lower-frequency region, represents the diffusion-limited process. With the dinitrospiropyran monolayer state of the electrode (**2a**), a higher resistance to interfacial electron transfer to the bioelectrocatalyst is observed, curve b, as compared to the protonated dinitromerocyanine monolayer electrode, curve a, that shows a smaller semicircle in the impedance spectrum, indicative of lower electron-transfer resistance. This is consistent with the fact that Fc-GOx is negatively charged at pH = 7.0 (isoelectric point, pI = 4) (*30*). With the neutral dinitrospiropyran monolayer electrode (**2a**-state), no affinity interactions between the bioelectrocatalyst and the modified electrode exist and a typical interfacial electron-transfer resistance for the electrooxidation of the redox probe by the functionalized electrode is observed. Photoisomerization of the monolayer to the protonated dinitromerocyanine monolayer state leads to the electrostatic attraction of the negatively charged Fc-GOx to the electrode surface. Concentration of Fc-GOx at the electrode surface facilitates interfacial electron transfer. This is accompanied by the lowering of the electron-transfer resistance at the electrode−solution interface, reflected by the smaller diameter of the semicircle region of the resulting impedance spectrum, Figure 3, curve a. In the presence of added DNP-Ab to the protonated dinitromerocyanine monolayer electrode, the impedance spectrum is almost unaffected, suggesting that the antibody does not bind to the monolayer interface. The dinitrospiropyran (**2a**)-monolayer electrode, however, shows a dramatic increase in the impedance spectrum upon interaction with the DNP-Ab, Figure 3, curve c. The semicircle region of the spectrum is so large that it appears as a straight line, and the corresponding R_{et} is so high that it cannot be evaluated from the plot. The tremendous increase in the R_{et} value upon the association of the DNP-Ab to the **2a**-monolayer-functionalized electrode is attributed to the insulation of the electrode surface that prohibits interfacial electron transfer. Photoisomerization of the monolayer to the dinitromerocyanine (**2b**)-monolayer states, followed by washing-off of the antibody, restores the impedance spectrum of the **2b**-monolayer electrode shown in Figure 3, curve a. The dissociation of the DNP-Ab from the **2b**-monolayer-functionalized electrode allows the cyclic impedance transduction of the photoisomerization reaction at the monolayer electrode, as well as the reversible binding/dissociation of the DNP-Ab to and from the photoisomerizable antigen interface, respectively. Figure 4A shows the cyclic Faradaic impedance probing of the photoisomerizable monolayer electrode using Fc-GOx/glucose as redox probe. With the **2b**-monolayer electrode, a lower electron-transfer resistance, R_{et} = ca. 1.2 MΩ, is induced, whereas with the dinitrospiropyran (**2a**)-monolayer electrode, a high electron-transfer resistance, R_{et} = ca. 2 MΩ, is observed. For the system that involves the association/dissociation of the DNP-Ab upon photoisomerization of the monolayer, the reversible Faradaic impedance transduction of the antibody binding dissociation events cannot be transduced by the R_{et} value of the system, because this value cannot be determined in the presence of the **2a**-DNP-Ab complex as a result of the very high interfacial electron-transfer resistance. The different events at the electrode interface, however, can be transduced by Faradaic signals by the recording of the Z_{im} value of the system at a constant Z_{re} value. Figure 4B shows the cyclic Faradaic impedance transduction signals reflecting the reversible sensing of the DNP-Ab and the cyclic regeneration of the sensing interface. The data were

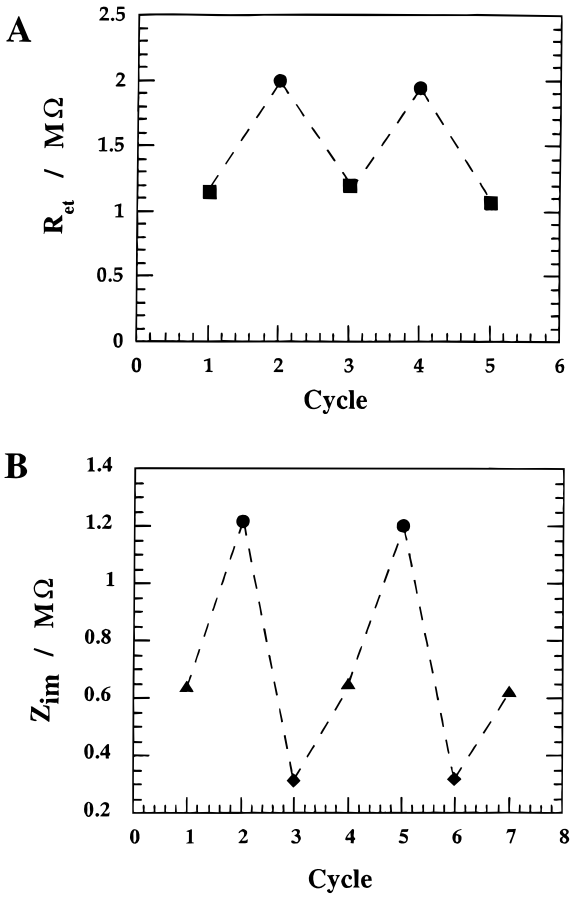

Figure 4. (A) Cyclic Faradaic impedance transduction of the photoisomerization of the dinitrospiropyran monolayer presented as the electron-transfer resistance, R_{et}: (■) protonated dinitromerocyanine (**2b**) monolayer and (●) dinitrospiropyran (**2a**) monolayer. (B) Cyclic Faradaic impedance transduction of the photoswitchable interactions of the DNP-Ab with the photoisomerizable monolayer electrode, presented as Z_{im} measured at $Z_{re} = 0.6$ MΩ, R_{et}: (▲) **2a**-monolayer, (●) **2a**-monolayer in the presence of DNP-Ab, and (◆) monolayer in the **2b**-state and DNP-Ab washed off. In all experiments, Fc-GOx, 3 mg mL^{-1}, and glucose were used as a redox probe. Measurements were performed with an applied bias potential of 0.4 V and an alternating voltage amplitude of 10 mV.

presented for a $Z_{re} = 0.7$ MΩ value. The **2a**-monolayer electrode, corresponding to the sensing interface, reveals the $Z_{im} = 0.65$ MΩ value. Interaction of the sensing electrode with the DNP-Ab increases Z_{im} to 1.0 MΩ, indicating the association of the antibody to the interface and increase of the electron-transfer resistance. Photoisomerization of the monolayer to the **2b**-state, followed by rinsing of the antibody, generates the $Z_{im} = 0.38$ MΩ value, indicating that the DNP-Ab was washed off and the electrostatic attraction of the bioelectrocatalytic probe to the functionalized electrode facilitates interfacial electron transfer. Subsequent photoisomerization of the **2b**-monolayer electrode to the **2a**-functionalized electrodes restores the sensing interface, $Z_{im} = 0.7$ MΩ. By cyclic photoisomerization of the monolayer between the **2a** and **2b** photoisomer states, the sensing interface is regenerated and the DNP-Ab is reversibly sensed using Faradaic impedance spectroscopy, Scheme 7 and Figure 4B.

The photochemically controlled interfacial electron-transfer resistance at the functionalized electrode upon formation or dissociation of the antigen−antibody complex suggests that the amperometric transduction of the

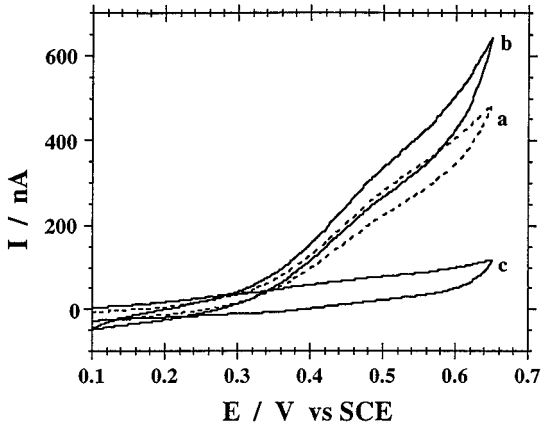

Figure 5. Cyclic voltammograms of the photoisomerizable monolayer in the presence of Fc-GOx, 3 mg mL^{-1}, and glucose, 1×10^{-4} M: (a) **2a**-monolayer electrode, (b) **2b**-monolayer electrode, (c) **2a**-monolayer electrode in the presence of DNP-Ab. All experiments were performed in a 0.01 M phosphate buffer solution, pH = 7.0, with a scan rate of 2 mV s^{-1}.

bioaffinity interactions could provide an alternative method to electronically transduce the photoswitchable antigen−antibody interactions. Binding of the DNP-Ab to the **2a**-functionalized electrode is expected to block the electrical contact between Fc-GOx and the electrode, leading to the inhibition of the bioelectrocatalyzed oxidation of glucose. The lack of binding of DNP-Ab to the **2b**-dinitrospiropyran-monolayer electrode, or the dissociation of the antibody from the **2b**-monolayer electrode, would facilitate the electrical contact between Fc-GOx and the electrode and activate the enzyme for the bioelectrocatalyzed oxidation of glucose. Thus, the binding or dissociation of the DNP-Ab to and from the photoisomerizable monolayer electrode is reflected by the current transduced by the electrode that is controlled by the activated or blocked bioelectrocatalytic activation of the Fc-GOx/glucose system. Figure 5 shows the cyclic voltammograms of the dinitrospiropyran photoisomerizable monolayer in the absence and the presence of the DNP-Ab, with Fc-GOx/glucose as a redox probe in the solution. The cyclic voltammograms of the **2a**-functionalized electrode, curve a, and the **2b**-modified Au-electrode, curve b, are almost identical and reveal the effective bioelectrocatalyzed oxidation of glucose by Fc-GOx, a process that is reflected by the electrocatalytic anodic current. The slight enhanced amperometric response of the Fc-GOx/glucose system at the **2b**-modified electrode is attributed to the electrostatic attraction of the biocatalyst by the positively charged interface. This results in the enhanced electrical communication between the biocatalyst and the electrode, consistent with our previous conclusions based on Faradaic impedance spectroscopy. Treatment of the photoisomerizable monolayer electrode with the DNP-Ab results in the complete blockage of the amperometric response of the **2a**-dinitrospiropyran-monolayer electrode, curve c, while the current response of the **2b**-functionalized electrode is almost unchanged in the presence of the DNP-Ab. These results demonstrate that binding of the DNP-Ab to the **2a**-antigen-monolayer electrode prevents the electrical contact between Fc-GOx and the electrode, resulting in the inhibition of the bioelectrocatalyzed oxidation of glucose. Because the DNP-Ab does not associate with the protonated dinitromerocyanine (**2b**) monolayer, the interfacial electrical contact between Fc-GOx and the electrode is not perturbed, and the bioelectrocatalyzed oxidation of glucose proceeds. The amperometric responses of the photo-

isomerizable electrode in the presence of the DNP-Ab and Fc-GOx/glucose system enables us to electrochemically probe the reversible sensing of the antibody and the photochemical regeneration of the sensing interface, Scheme 7 and Figure 5. In the presence of the **2a**-functionalized electrode and the DNP-Ab, the bioelectrocatalyzed oxidation of glucose by Fc-GOx is switched-off, indicating the specific association of the antibody to the electrode support. Photoisomerization of the resulting electrode to the **2b**-monolayer state, followed by the washing-off of the antibody, activates the bioelectrocatalyzed oxidation of glucose, and a high amperometric response is detected. Further photoisomerization of the monolayer-functionalized-electrode to the dinitrospiropyran (**2a**) state regenerates the sensing interface, and the DNP-Ab insulates the electrode support in a second cycle. By the cyclic photoisomerization of the monolayer interface between the **2b** and **2a** states, the antibody can be washed-off, and the sensing interface is regenerated, respectively.

In the previous examples, the light-stimulated affinity interactions between the DNP-Ab and the photoisomerizable monolayer interface and the interfacial electron-transfer properties at the modified electrode were controlled by the associative/dissociative interactions between the antibody and the electrode. Accordingly, the transducer reflecting the photoswitchable binding interactions was an electrode, and amperometric or impedance signals were used to probe the chemical events at the conductive support. A different electronic transduction means of the photoswitchable bioaffinity interactions between the antibody and the photoisomerizable interface is the microgravimetric, piezoelectrical quartz crystal microbalance (QCM) analysis. The use of piezoelectric quartz crystals for the microgravimetric QCM analysis of antigen−antibody interactions has been addressed in several reports (*12*). The frequency change of a quartz crystal, Δf, upon a mass alteration of Δm occurring on the crystal, is given by eq 5, where f_o is the fundamental frequency

$$\Delta f = -\left[\frac{2nf_o^2}{(\mu_q \rho_q)^{1/2}}\right]\Delta M = -C_f \Delta m = -1.83 \times 10^8 \text{ (Hz cm}^2\text{ g}^{-1})\Delta m \quad (5)$$

of the crystal, n is the overtone number ($n = 1$), ρ_q is the density of quartz (2.65 g cm^{-2}), and μ_q is the shear modulus of quartz (2.95×10^{11} dyne cm^{-2}). For the quartz crystals used in our study (AT-cut, 9 MHz) $C_f = 1.83 \times 10^8$ (Hz cm^2 g^{-1}). Thus, the mass changes occurring on the crystal as a result of the binding or dissociation of the DNP-Ab are expected to be transduced as frequency changes of the crystal. Thus, the association of the antibody to the **2a**-functionalized piezoelectric crystal is anticipated to stimulate a decrease in the crystal frequency, whereas the dissociation of the DNP-Ab upon photoisomerization of the monolayer to the **2b**-photoisomer state induces a frequency increase due to a mass loss, Scheme 6.

The Au-electrodes supported onto the quartz crystal were modified by the thiolated dinitrospiropyran (**2a**) photoisomerizable monolayer, Scheme 6. Immobilization of **2a** onto the Au−quartz crystal results in a crystal frequency change of $\Delta f = -150$ Hz that translates to a surface coverage of ca. 3×10^9 mol cm^{-2} of the photoisomerizable antigen on the Au support. Figure 6A shows the time-dependent crystal frequency changes upon interaction of the dinitrospiropyran (**2a**)-monolayer-functionalized crystal with the DNP-Ab, curve a, and upon

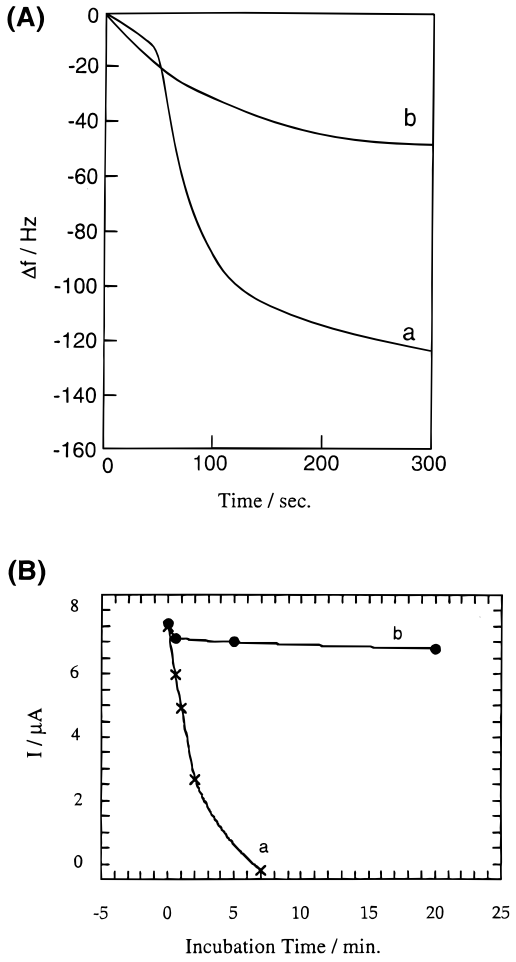

Figure 6. (A) Time-dependent frequency changes of the photoisomerizable monolayer-modified Au quartz crystal upon interaction with the DNP-Ab, 30 μg mL^{-1}: (a) **2a**-monolayer-functionalized crystal and (b) **2b**-monolayer-functionalized crystal. (B) Time-dependent amperometric responses of the photoisomerizable monolayer electrode upon interaction with the DNP-Ab, 50 μg mL^{-1}, using Fc-GOx, 5 mg·mL^{-1}, and glucose, 5 $\times 10^{-2}$ M, in phosphate buffer, pH = 7.0, as a redox probe; scan rate 5 mV s^{-1} (amperometric responses measured at the peak of anodic current): (a) **2a**-monolayer electrode and (b) **2b**-monolayer electrode.

treatment of the protonated dinitromerocyanine interface (**2b**) with the antibody, curve b. With the **2a**-functionalized crystal, a time-dependent decrease in the frequency is observed, consistent with the association of the antibody onto the antigen-functionalized surface. The frequency drop levels off to a value of ca. $\Delta f = -120$ Hz that represents the equilibrated state of the antigen−antibody bioaffinity complex on the surface. Interaction of the **2b**-modified electrode with the DNP-Ab results in the frequency drop shown in Figure 6A, curve b. A substantial smaller drop in crystal frequency is observed. Washing of the cell with the buffer solution does not affect the frequency drop observed with the **2a**-monolayer/DNP-Ab system, whereas the frequency of the **2b**-monolayer/DNP-Ab assembly is almost recovered to the initial crystal frequency (defined as zero frequency). Thus, the drop in the **2b**-crystal is attributed to the nonspecific adsorption of DNP-Ab to the interface. This nonspecific protein adsorbate is easily washed off, whereas the specific association of the DNP-Ab to the **2a**-modified crystal is unaffected by the rinsing process. The frequency change observed upon the association of the DNP-Ab to the **2a**-functionalized crystal, $\Delta f \approx -120$ Hz, corresponds

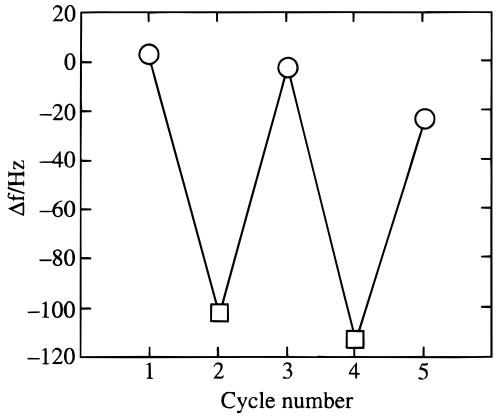

Figure 7. Cyclic microgravimetric QCM analysis of the interactions of DNP-Ab with the photoisomerizable monolayer-functionalized Au crystal: frequency of (○) protonated dinitromerocyanine (**2b**) monolayer after rinsing off the DNP-Ab and (□) dinitrospiropyran (**2a**) monolayer, after interaction with DNP-Ab, 10 μg mL^{-1}, for 10 min. (The *X*-axis corresponds to the cycle number).

to a surface coverage of the monolayer by the antibody of ca. 4.1 × 10^{-12} mol cm^{-2}. The dynamics of the association of the DNP-Ab to the **2a**- and **2b**-modified crystal is fully consistent with the characterization of the time-dependent binding of the antibody in the photoisomerizable surfaces using Fc-GOx/glucose as redox probe, Figure 6B. Interaction of the **2b**-dinitromerocyanine monolayer electrode with the DNP-Ab does not inhibit the bioelectrocatalyzed oxidation of glucose, implying the lack of antibody binding to the surface, Figure 6B, curve (b). The slight initial decrease in the current could be attributed to the nonspecific association of the protein on the electrode. Interaction of the **2a**-modified electrode yields a time-dependent insulation of the bioelectrocatalyzed oxidation of glucose, Figure 6B, curve (a), in agreement with the specific binding of the antibody to the antigen interface. The time constants for the binding of the DNP-Ab to the **2a**-antigen-monolayer in the microgravimetric QCM study and the electrochemical experiments are similar, and within 5 min, ca. 85−90% of the Ab is linked to the surface.

Similarly to the electrochemical systems, the microgravimetric QCM method allows the electronic transduction of the sensing process by the **2a**-monolayer- functionalized crystal and the regeneration and reuse of the immunosensor interface, Figure 7. Binding of DNP-Ab to the dinitrospiropyran (**2a**) monolayer results in a decrease in the crystal frequency upon interaction with DNP-Ab. Photoisomerization of the interface to the **2b**-photoisomer state, followed by rinsing of the electrode, restores the original crystal frequency, indicating that the sensed antibody had been washed off. By subsequent photoisomerization of the monolayer to the **2a**-configuration, the DNP-Ab can be sensed again. Thus, by a two-step irradiation process that includes the intermediary rinsing off of the antibody, the cyclic regeneration of the antibody-sensing interface is accomplished.

The photostimulated binding and dissociation of antibodies to and from photoisomerizable antigen interfaces, respectively, and the regeneration of the immunosensing interface represents a major advance in immunosensor technology. The available immunosensors are single-cycle analytical systems. The approach to regenerate the sensing interface through the application of photoisomerizable antigens could be developed into a general method for tailoring reusable immunosensors.

Conclusions

Optoelectronic systems for the amperometric transduction of photonic information and for immunosensor applications were described. The systems were organized by the assembly of photoisomerizable monolayers on Au-electrodes acting as "photocommand interfaces" for controlling the functions of the biomaterials and their resulting electron responses in the presence of the electronic transducer. The electrical contact of cytochrome *c* with an electrode was controlled by a functionalization of the conductive support with a photoisomerizable monolayer. The light-stimulated electrical communication of the hemoprotein and the electrode was amplified by the coupling of Cyt *c* to the secondary bioelectrocatalyzed reduction of O_2 in the presence of cytochrome oxidase. The system was used for the amplified amperometric transduction of recorded photonic signals. The optobioelectronically based immunosensor systems revealed light-controlled antigen−antibody interactions at a photoisomerizable antigen-monolayer electrode. We have addressed three different means to transduce the light-stimulated affinity interactions at the electrode support, including impedance spectroscopy, amperometric cyclic voltammetry, and microgravimetric quartz crystal microbalance piezoelectric analyses. All methods provided means to characterize different basic aspects associated with the formation or dissociation of the antigen−antibody complexes at the transducer. All three methods complement and agree with each other in respect to the transduction of the bioevents that involve the binding or the dissociation of the DNP-Ab to or from the photoisomerizable interface, respectively.

The recording of the photonic signals occurs by a two-dimensional photoisomerizable layer of molecular thickness associated with the transducer. The rapid progress in the development of nanoscopic scanning light sources, e.g., near-field optical microscopy, suggests that encoding of optical information in the two-dimensional photoactive array could lead to dense information storage assemblies that can be read out by the electronic response of the transducer support. Alternatively, the nanoscale lateral photochemical encoding of the recognition features between the antibody and the photoisomerizable antigen could be used to pattern interfaces with various and different biomaterials. That is, the labeling of different biomaterials with the DNP-Ab conjugate could be applied for the light-induced micro- and nanoscale patterning of the biomaterials and the generation of new classes of "biochips".

Acknowledgment

This research was supported by THE ISRAEL SCIENCE FOUNDATION founded by The Israel Academy of Sciences and Humanities.

References and Notes

(1) (a) Willner, I.; Katz, E.; Willner, B. Electrical Contact of Redox Enzyme Layers Associated with Electrodes: Routes to Amperometric Biosensors. *Electroanalysis* **1997**, *9*, 965−977. (b) Katz, E.; Heleg-Shabtai, V.; Willner, B.; Willner, I.; Bückmann, A. F. Electrical Contact of Redox Enzymes with Electrodes: Novel Approaches for Amperometric Biosensors. *Bioelectrochem. Bioenerg.* **1997**, *42*, 95−104. (c) Skládal, P. Advances in Electrochemical Immunosensors. *Electroanalysis* **1997**, *9*, 737−745. (d) Ghindilis, A. L.; Atanasov, P.; Wilkins, M.; Wilkins, E. Immunosensors: Electrochemical Sensing and Other Engineering Approaches. *Biosens. Bioelectron.* **1998**, *13*, 113−131.

(2) (a) Göpel, W.; Heiduschka, P. Introduction to Bioelectronics: Interfacing Biology with Electronics. *Biosens. Bioelectron.* **1994**, *9*, iii−xiii. (b) Willner, I.; Katz, E.; Willner, B.; Blonder, R.; Heleg-Shabtai, V.; Bückmann, A. F. Assembly of Functionalized Monolayers of Redox Proteins on Electrode Surfaces: Novel Bioelectronic and Optoelectronic Systems. *Biosens. Bioelectron.* **1997**, *12*, 337−356. (c) Schmidt, H.-L.; Schuhmann, W. Reagentless Oxidoreductase Sensors. *Biosens. Bioelectron.* **1996**, *11*, 127−135. (d) Bartlett, P. N. Application of Enzymes in Amperometric Sensors: Problems and Possibilities. In *Biosensor Technology. Fundamentals and Applications*; Buck, R. P., Hatfield, W. E., Umana, M., Bowden, E. F., Eds.; Marcel Dekker: New York, 1990; Chapter 7, pp 95−115.

(3) (a) Heller, A. Electrical Wiring of Redox Enzymes. *Acc. Chem. Res.* **1990**, *23*, 128−134. (b) Gregg, B. A.; Heller, A. Redox Polymer Films Containing Enzymes. 1. A Redox-Containing Epoxy Cement: Synthesis, Characterization, and Electrocatalytic Oxidation of Hydroquinone. *J. Phys. Chem.* **1991**, *95*, 5970−5975. (c) Heller, A. Electrical Connection of Enzyme Redox Centers to Electrodes. *J. Phys. Chem.* **1992**, *96*, 3579−3587.

(4) (a) Hale, P. D.; Inagaki, T.; Karan, H. I.; Okamoto, Y.; Skotheim, T. A. A New Class of Amperometric Biosensor Incorporating a Polymeric Electron-Transfer Mediator. *J. Am. Chem. Soc.* **1989**, *11*, 3482−3484. (b) Willner, I.; Lapidot, N.; Riklin, A.; Kasher, R.; Zahavy, E.; Katz, E. Electron-Transfer Communication in Glutathione Reductase Assemblies: Electrocatalytic, Photocatalytic and Catalytic Systems for the Reduction of Oxidized Glutathione. *J. Am. Chem. Soc.* **1994**, *116*, 1428−1441.

(5) (a) Willner, I.; Riklin, A.; Shoham, B.; Rivenzon, D.; Katz, E. Development of Novel Biosensor Enzyme Electrodes: Glucose Oxidase Multilayer Arrays Immobilized onto Self-Assembled Monolayers on Electrodes. *Adv. Mater.* **1993**, *5*, 912−915. (b) Riklin, A.; Willner, I. Glucose and Acetylcholine Sensing Multilayer Enzyme Electrodes of Controlled Enzyme Layer Thickness. *Anal. Chem.* **1995**, *67*, 4118−4126.

(6) (a) Willner, I.; Heleg-Shabtai, V.; Blonder, R.; Katz, E.; Tao, G.; Bückmann, A. F.; Heller, A. Electrical Wiring of Glucose Oxidase by Reconstitution of FAD-Modified Monolayers Assembled onto Au-Electrodes. *J. Am. Chem. Soc.* **1996**, *118*, 10321−10322. (b) Bardea, A.; Katz, E.; Bückmann, A. F.; Willner, I. Reconstituted-NAD^+- Dependent-Enzyme Electrodes: Electrical Contact of Cofactor-Dependent Enzymes and Electrodes. *J. Am. Chem. Soc.* **1997**, *119*, 9114−9119. (c) Heleg-Shabtai, V.; Katz, E.; Willner, I. Assembly of Microperoxidase-11 and Co(II)-Protoporphyrin IX Reconstituted Myoglobin Monolayers on Au-Electrodes: Integrated Bioelectrocatalytic Interfaces. *J. Am. Chem. Soc.* **1997**, *119*, 8121−8122.

(7) Katz, E.; Willner, I. Amperometric Amplification of Antigen-Antiobody Association at Monolayer Interfaces: Design of Immunosensor Electrodes. *J. Electroanal. Chem.* **1996**, *418*, 67−72.

(8) Blonder, R.; Katz, E.; Cohen, Y.; Itzhak, N.; Riklin, A.; Willner, I. Application of Redox Enzymes for Probing the Antigen−Antibody Association at Monolayer Interfaces: Development of Amperometric Immunosensor Electrodes. *Anal. Chem.* **1996**, *68*, 3151−3157.

(9) (a) Másson, M.; Yun, K.; Haruyama, T.; Kobatake, E.; Aizawa, M. Quartz Crystal Microbalance Bioaffinity Sensor for Biotin. *Anal. Chem.* **1995**, *67*, 2212−2215. (b) Suleiman, A. A.; Guilbault, G. G. Recent Developments in Piezoelectric Immunosensors. *Analyst* **1994**, *119*, 2279−2282.

(10) Ben-Dov, I.; Willner, I.; Zisman, E. Piezoelectric Immunosensors for Urine Specimens of *Chlamydia trachomatis* Employing Quartz-Crystal- Microbalance Microgravimetric Analyses. *Anal. Chem.* **1997**, *69*, 3506−3512.

(11) (a) Millan, K. M.; Mikkelsen, S. R. Sequence-Selective Biosensor for DNA Based on Electroactive Hybridization Indicators. *Anal. Chem.* **1993**, *65*, 2317−2323. (b) Hashimoto, K.; Ito, K.; Ishimori, Y. Sequence-Specific Gene Detection with a Gold Electrode Modified with DNA Probes and an Electrochemically Active Dye. *Anal. Chem.* **1994**, *66*, 3830−3833.

(12) (a) Bardea, A.; Dagan, A.; Ben-Dov, I.; Amit, B.; Willner, I. Amplified Microgravimetric Quartz-Crystal-Microbalance Analyses of Oligonucleotide Complexes: A Route to a Tay-Sachs Biosensor Device. *Chem. Commun.* **1998**, 839−840. (b) Ito, K.; Hashimoto, K.; Ishimori, Y. Quantitative Analysis for Solid-Phase Hybridization Reaction and Binding Reaction of DNA Binder to Hybrids Using a Quartz Crystal Microbalance. *Anal. Chim. Acta* **1996**, *327*, 29−35. (c) Caruso, F.; Rodda, E.; Furlong, D. N. Quartz Crystal Microbalance Study of DNA Immobilization and Hybridization for Nucleic Acid Sensor Development. *Anal. Chem.* **1997**, *69*, 2043−2049.

(13) (a) Lion-Dagan, M.; Katz, E.; Willner, I. Amperometric Transduction of Optical Signals Recorded by Organized Monolayers of Photoisomerizable Biomaterials on Au-electrodes. *J. Am. Chem. Soc.* **1994**, *116*, 7913−7914. (b) Willner, I.; Lion-Dagan, M.; Marx-Tibbon, S.; Katz, E. Bioelectrocatalyzed Amperometric Transduction of Recorded Optical Signals Using Monolayer-Modified Au-Electrodes. *J. Am. Chem. Soc.* **1995**, *117*, 6581−6592.

(14) (a) Willner, I.; Blonder, R.; Katz, E.; Stocker, A.; Bückmann, A. F. Reconstitution of Apo-Glucose Oxidase with a Nitrospiropyran-Modified FAD Cofactor Yields a Photoswitchable Biocatalyst for Amperometric Transduction of Recorded Optical Signals. *J. Am. Chem. Soc.* **1996**, *118*, 5310−5311. (b) Blonder, R.; Katz, E.; Willner, I.; Wray, V.; Bückmann, A. F. Application of a Nitrospiropyran-FAD Reconstituted Glucose Oxidase and Charged Electron Mediators as Optobioelectronic Assemblies for the Amperometric Transduction of Recorded Optical Signals: Control of the "ON"−"OFF" Direction of the Photoswitch. *J. Am. Chem. Soc.* **1997**, *119*, 11747−11757.

(15) Willner, I.; Doron, A.; Katz, E.; Levi, S.; Frank, A. J. Reversible Associative and Dissociative Interactions of Glucose Oxidase with Nitrospiropyran Monolayers Assembled onto Au-electrodes: Amperometric Transduction of Recorded Optical Signals. *Langmuir* **1996**, *12*, 946−954.

(16) Patolsky, F.; Filanovsky, B.; Katz, E.; Willner, I. Photoswitchable Antigen−Antibody Interactions Studied by Impedance Spectroscopy. *J. Phys. Chem. B* **1998**, *102*, 10359−10367.

(17) Allen, P. M.; Hill, H. A. O.; Walton, N. J. Surface Modifiers for the Promotion of Direct Electrochemistry of Cytochrome *c*. *J. Electroanal. Chem.* **1984**, *178*, 69−86.

(18) Frew, J. E.; Hill, H. A. O. Direct and Indirect Electron Transfer between Electrodes and Redox Proteins. *Eur. J. Biochem.* **1988**, *172*, 261−269.

(19) (a) Armstrong, F. A.; Hill, H. A. O.; Walton, N. J. Reactions of Electron-Transfer Proteins at Electrodes. *Quart. Rev. Biophys.* **1985**, *18*, 261−322. (b) Eddowes, M. J.; Hill, H. A. O. Novel Method for the Investigation of the Electrochemistry of Metalloproteins: Cytochrome *c*. *J. Chem. Soc., Chem. Commun.* **1977**, 771−772.

(20) Eddowes, M. J.; Hill, H. A. O.; Uosaki, K. The Electrochemistry of Cytochrome *c*. Investigation of the Mechanism of the 4,4′-Bipyridyl Surface Modified Gold Electrode. *Bioelectrochem. Bioenerg.* **1980**, *7*, 527−537.

(21) Barlow, G. H.; Margoliash, E. Electrophoretic Behavior of Mammalian-Type Cytochrome *c*. *J. Biol. Chem.* **1966**, *241*, 1473−1477.

(22) (a) Lion-Dagan, M.; Katz, E.; Willner, I. A Bifunctional Monolayer Electrode Consisting of 4-Pyridyl Sulfide and Photoisomerizable Spiropyran. Photoswitchable Electrical Communication between the Electrode and Cytochrome *c*. *J. Chem. Soc., Chem. Commun.* **1994**, 2741−2742. (b) Lion-Dagan, M.; Ben-Dov, I.; Willner, I. Microgravimetric Quartz-Crystal-Microbalance Analysis of Cytochrome *c* Interactions with Pyridine and Pyridine-Nitrospiropyran Monoalyer Electrodes and Characterization of Inter-Protein Complexes at the Functionalized Surfaces. *Colloids Surf., B* **1997**, *8*, 251−260.

(23) (a) Willner, I.; Blonder, R.; Dagan, A. Application of Photoisomerizable Antigenic Monolayer-electrodes as Reversible Amperometric Immunosensors. *J. Am. Chem. Soc.* **1994**, *116*, 9365−9366. (b) Blonder, R.; Ben-Dov, I.; Dagan, A.; Willner, I.; Zisman, E. Photochemically-Activated Electrodes: Application in Design of Reversible Immunosensors

and Antibody Patterned Interfaces. *Biosens. Bioelectron.* **1997**, *12*, 627−644.
(24) Blonder, R.; Levi, S.; Tao, G.; Ben-Dov, I.; Willner, I. Development of Amperometric and Microgravimetric Immunosensors and Reversible Immunosensors Using Antigen and Photoisomerizable Antigen Monolayer Electrodes. *J. Am. Chem. Soc.* **1997**, *119*, 10467−10478.
(25) Bard, A. J.; Faulkner, L. R. *Electrochemical Methods: Fundamental and Applications;* Wiley: New York, 1980.
(26) Stoynov, Z. B.; Grafov, B. M.; Savova-Stoynov, B. S.; Elkin, V. V. *Electrochemical Impedance*; Nauka Publisher: Moscow, 1991.
(27) (a) Knichel, M.; Heiduschka, P.; Beck, W.; Jung, G.; Göpel, W. Utilization of a Self-Assembled Peptide Monolayer for an Impedimetric Immunosensor. *Sens. Actuators B* **1995**, *B28*, 85−94. (b) Rickert, J.; Göpel, W.; Beck, W.; Jung, G.; Heiduschka, P. A "Mixed" Self-Assembled Monolayer for an Impedimetric Immunosensor. *Biosens. Bioelectron.* **1996**, *11*, 757−768.
(28) Athey, D.; Ball, M.; McNeil, C. J.; Armstrong, R. D. A Study of Enzyme-Catalyzed Product Deposition on Planar Gold Electrodes Using Electrical Impedance Measurement. *Electroanalysis* **1995**, *7*, 270−273.
(29) Degani, Y.; Heller, A. Direct Electrical Communication between Chemically Modified Enzymes and Metal Electrodes. 1. Electron Transfer from Glucose Oxidase to Metal Electrodes via Electron Relays, Bound Covalently to the Enzyme. *J. Phys. Chem.* **1987**, *91*, 1285−1289.
(30) Wilson, R.; Turner, A. P. F. Glucose Oxidase: An Ideal Enzyme. *Biosens. Bioelectron.* **1992**, *7*, 165−185.

Accepted September 14, 1999.

BP990115A